Iranian Journal of Astronomy and Astrophysics
Vol. 12, No. 3, Summer 2025, 291–297
©Available online at http://ijaa.du.ac.ir
DOI: 10.22128/ijaa.2026.3131.1228
Online ISSN: 2383–403X

Iranian Journal of Astronomy and Astrophysics

Research Paper

Solar Wind–Geomagnetic Coupling Based on Yearly Averages

Balveer S Rathore*[1] · Nidhi Parmar[2]
[1] Government Holkar Science College, Indore, M.P. India;
*E-mail: balveer.rathor@gmail.com
[2] Government Holkar Science College, Indore, M.P. India;
E-mail: nidhiparmar@collegeholkar.org

Received: 10 November 2025; **Accepted:** 21 January 2026; **Published:** 8 February 2026

Abstract. Understanding solar phenomena is essential for predicting and mitigating the effects of solar activity on Earth's near-space environment. Solar variability influences space weather conditions, impacting satellite operations, communication systems, and even terrestrial climate. Continuous investigation into the dynamic relationship between solar and geomagnetic parameters provides valuable insight into the Sun–Earth connection. Future work in solar phenomena research will likely focus on improving our understanding of the Sun's behaviors, particularly regarding its impact on Earth. This includes refining and investigating the connection between solar activity and terrestrial climate. In the present work, the focus is on examining the relationship between solar wind parameters and geomagnetic indices using yearly averaged data. The electric field and IMF Bz vary noticeably, exhibiting peaks that correspond with sunspot cycles (spanning the years 2014 to 2025). The total magnetic field B increases during solar maxima and shows a strong correlation with the Dst index. The Dst index becomes more negative during periods of high sunspot activity, indicating stronger geomagnetic storms during the observed duration. Bz shows fluctuations between positive and negative values with no clear long-term trend. The negative Bz (southward) component is essential because it couples strongly with Earth's magnetosphere, enhancing geomagnetic storms.

Keywords: Solar Cycle, Sun Spots, Solar wind, Geomagnetic Storms.

1 Introduction

The Airbus public communiqué states that an analysis of a recent event involving an A320 family aircraft has revealed that intense solar radiation may corrupt data critical to the functioning of flight controls. on the date 30 October 2025. "Intense solar radiation" refers to solar activity such as solar flares or coronal mass ejections, which can produce high-energy particles. These particles can cause single-event upsets (SEUs) in electronic components—momentary bit flips or corrupted data in computer systems. This news attracts everyone to learn about solar radiation and its effects on aviation as well as navigation systems. Many researchers address this problem [1–4]. This solar radiation affects Earth's magnetosphere. Disturbance in Earth's magnetosphere is known as a geomagnetic storm [4–7].

* *Corresponding author*

Geomagnetic storms typically arise from disturbances in the IMF and solar wind plasma emissions, often triggered by solar phenomena such as coronal mass ejections (CMEs) and solar flares [8,9]. Understanding these global disruptions in Earth's magnetic field is fundamental to solar-terrestrial physics, as GMSs can produce severe consequences, including power grid failures, satellite malfunctions, communication disruptions, and navigation errors [8,9]. Taran, Somayeh, et al. investigated "Effect of geomagnetic storms on a power network at mid latitudes." The study published in Advances in Space Research, addressed the fast solar wind problem [9,10].

Several mechanisms have been proposed to explain how enhanced solar wind–magnetosphere coupling [11,12].

contributes to GMS development. Dungey (1961) introduced the concept of magnetic reconnection at the dayside magnetopause, where Earth's magnetic field interacts with the southward component of the IMF [13]. This reconnection lets particles from the solar wind into the magnetosphere, which creates a neutral point in the magnetotail. The subsequent injection of high-energy particles leads to the generation of a ring current, which weakens the geomagnetic field, an effect quantified by the Disturbance Storm Time (Dst) index. Meanwhile, lower-energy particles follow stretched field lines toward the polar regions, where they collide with the upper atmosphere, enhancing auroral activity [13].

Research has consistently shown that solar wind plasma parameters play a crucial role in influencing geomagnetic storms (GMSs). A notable study titled *"Effect of Solar Wind Plasma Parameters on Space Weather"* by Rathore et al. (2015) highlights that parameters such as the southward component of the interplanetary magnetic field (IMF Bz), the interplanetary electric field, and plasma temperature serve as reliable predictors of geomagnetic activity [14]. The study further emphasizes that the time delay between the maximum southward Bz and the minimum Dst index can be used to forecast the intensity of geomagnetic storms. Many more investigated similar problems in the last decade [8–14].

2 Data Analysis

Many research groups used hourly average data, but in this work, we have used a different approach; the yearly average of the parameters is used. A Comparative graph was generated using NASA OMNIWEB data (), using the parameters of Sunspots or Interplanetary solar wind.

1. Sunspot Number
2. B_{Total} (interplanetary magnetic field of solar wind)
3. Bz (southward component of magnetic field)
4. Solar Wind Proton Density (N/cm^3)
5. Electric Field (mV/m)
6. Dst Index (nT)

Dst Index (nT) is taken as a measure of depression in Earth's magnetic field near the equator, indicating geomagnetic storm strength. A critical value Dst $\leq$ -50nT is taken as an indicator of a Geomagnetic Storm.

Table 1: Yearly Average Data of geomagnetic storm (2009-2025).

Year	Sunspot	B Total	B_Z (nT GSM)	SW Proton density	E electric field	DST index
2009	5	3.9	0.1	5.9	-0.06	-3
2010	25	4.7	0.1	5.4	-0.04	-9
2011	81	5.3	0.2	5.2	-0.08	-11
2012	85	5.7	-0.3	5.6	0.12	-12
2013	94	5.2	-0.2	5.6	0.07	-10
2014	113	6.1	0.2	6.2	-0.12	-11
2015	70	6.7	-0.1	7.1	0.07	-21
2016	40	6.1	0	6.7	0.02	-12
2017	22	5.2	-0.1	6.4	0.09	-13
2018	7	4.7	-0.1	6.9	0.06	-8
2019	4	4.5	-0.2	6.4	0.07	-8
2020	9	4.3	-0.2	6.4	0.1	-8
2021	30	5	-0.1	6.7	0.04	-6
2022	83	6.4	0	5.7	0	-9
2023	125	6.5	-0.2	5.8	0.07	-12
2024	154	6.9	-0.1	7.1	0.03	-12
2025	144	7.7	-0.2	6.8	0.13	-17

3 Result and Observation

The availability of extensive historical datasets has energized research into geomagnetic index forecasting, often focusing on predicting hourly averaged indices a few hours in advance using a variety of mathematical and Machine Learning (ML) techniques [15–17]. Similar methodologies have also been applied to forecast the Dst index [18–20]. These approaches leverage real-time data to improve precision in short-term forecasts, which is crucial for timely responses to geomagnetic events.

Sunspot increases sharply from 2009 to a peak around 2014 (Solar Cycle 24 maximum), then declines until 2019 (solar minimum), followed by another strong rise toward 2024–2025 (Cycle 25). This curve reflects the 11-year solar cycle. Higher sunspot numbers indicate greater solar magnetic activity and stronger solar wind output. Magnetic field B follows a similar upward trend with solar activity, peaking during active years (2014–2015 and again in 2024–2025). The interplanetary magnetic field (IMF) becomes stronger during solar maxima, increasing the likelihood of geomagnetic disturbances. Bz shows fluctuations between positive and negative values with no clear long-term trend. The negative Bz (southward) component is essential because it couples strongly with Earth's magnetosphere, enhancing geomagnetic storms. This variable's irregular pattern indicates variable solar wind–magnetosphere coupling over the years. Solar wind Density shows moderate variations between $\sim$5 and 7 cm^{-3} with peaks around active years (2014–2015, 2024–2025). Denser solar wind flows are typically associated with increased solar wind dynamic pressure during active solar periods. Small positive and negative variations with some spikes (notably in 2012 and 2025) were observed in Electric Field E. The interplanetary electric field arises from solar wind–magnetic field interaction. Positive spikes may correspond to stronger coupling events between the solar wind and Earth's magnetosphere.

Dst Index was negative throughout (as expected). Stronger negative values (around 21 in 2015 and 17 in 2025) indicate geomagnetic storms. Periods of high solar and IMF activity (e.g., 2014–2015, 2025) show more negative Dst, confirming stronger geomagnetic disturbances.

Fig. 1 shows six subplots, each representing one solar–terrestrial parameter over the years 2009–2025. Together, they illustrate how solar activity and solar wind conditions

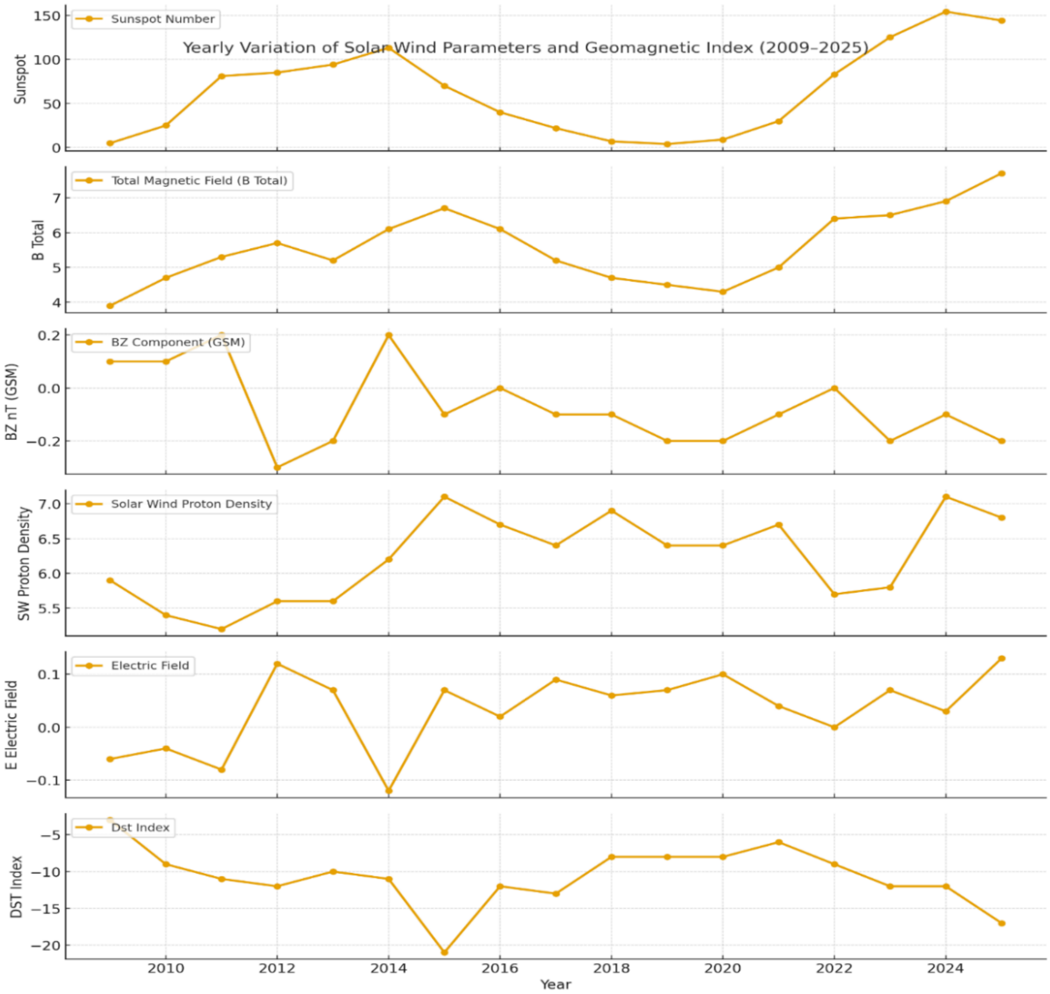

Figure 1: Solar–terrestrial parameter over the years 2009–2025.

change during Solar Cycle 24 and the onset of Cycle 25.

Table 2: Correlation and Regression coefficient of solar wind parameters with Dst.

Parameter	**Correlation coefficient r**	**Regression coefficient β**
Sun Spots Number	-0.53	+0.018
B-total	-0.77	**−3.51**
Bz	+0.21	**−19.01**
SW density	-0.35	+0.70
E-field	-0.35	**−50.32**

Table 2 shows the different statistical parameters, i.e., correlation coefficient, regression coefficient.

The correlation coefficient between Dst and sunspots is -0.53, which shows a moderate negative correlation. That means higher sunspot activity tends to be associated with more

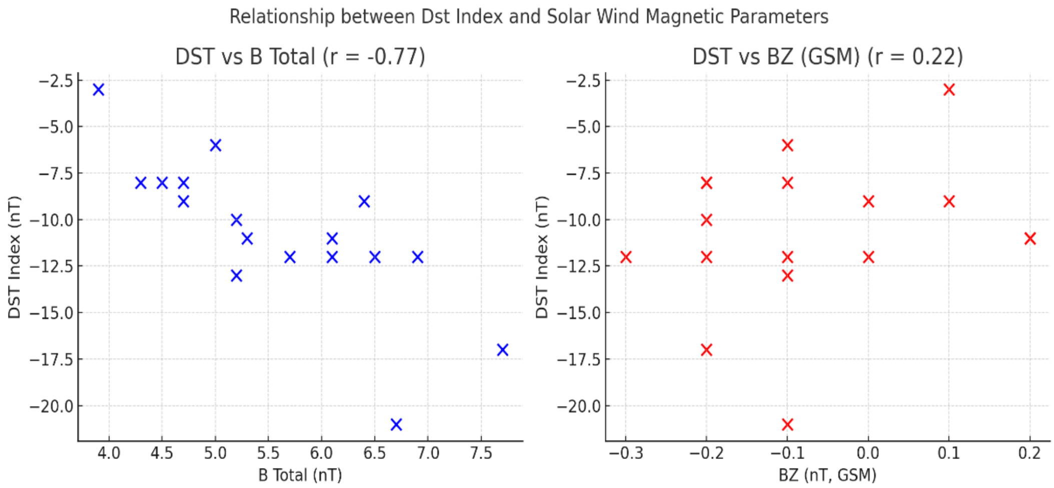

Figure 2: Relationship between Dst Index and Solar Wind Magnetic Parameters.

negative (stronger) Dst storms.

The correlation with B-total is -0.77, indicating a strong negative relationship. Therefore, a larger IMF magnitude is strongly linked to stronger geomagnetic storms. A p-value is, 3.29207×10^{-10} This is exceptionally strong evidence that the effect measured is real and not a statistical fluke.

Bz has a very weak positive correlation (+0.21). This is due to the dataset having only a few strong southward Bz cases, so the correlation is weak. Bz shows weak correlation due to dataset limitations. Although physically, the southward Bz is the *primary driver* of storm strength, yearly averages datasets smooth out short intervals of strong negative Bz. Hence, the correlation appears weak. But previous research has found a good correlation between Bz and Dst in hourly average datasets. Therefore, the time duration of southward turning is very important in storm triggering.

A correlation of -0.35 between solar wind density and the Electric field Ey has been found, indicating a weak, moderate negative correlation. That means higher density mildly favors stronger storms. Similarly, stronger solar wind E-field often drives stronger storms. Solar wind density and E-field show weaker correlations. Both have mild influence; E-field ($V \times B$) normally correlates strongly with storms, but annual averaging reduces the sensitivity

The analysis shows that among all parameters, B-total has the strongest negative correlation with the Dst index (r = -0.77), followed by sunspot number (r = -0.53), solar wind density (r = -0.35), and the electric field (r = -0.35), while Bz shows only a weak positive correlation (r = +0.21). However, regression coefficients reveal the true physical influence after controlling for multicollinearity: the electric field emerges as the most dominant predictor with a large negative effect (β = -50.32), indicating that even a small increase greatly depresses the Dst index. Bz also shows a strong negative regression coefficient (β = -19.01), consistent with the well-known role of southward IMF in storm intensification. B-total contributes moderately (β = -3.51), while sunspot number (β = +0.018) and solar wind density (β = +0.70) show weak positive effects in the multivariate model. Overall, correlation alone can be misleading—especially for Bz, while regression highlights that E-field and Bz are the primary drivers of Dst variability, with B-total also playing an important but secondary role.

4 Conclusion

This paper unequivocally shifts its focus to a comprehensive yearly analysis of the variation of solar parameters, building on the insights gained from previously available monthly data.

1. The Sunspot Number, B Total, and Solar Wind Density clearly follow solar cycle trends.
2. Bz, Electric Field, and Dst Index show how solar activity translates into geomagnetic effects.
3. Peaks in 2014–2015 and rising activity in 2024–2025 correspond to solar maximum phases, where geomagnetic disturbances (negative Dst) are more frequent and intense.

1. This suggests that Bz alone (averaged yearly) does not strongly predict Dst changes — but on shorter time scales, southward (negative) Bz components are known to drive geomagnetic activity.

Acknowledgment

The authors are thankful to the World Data Centre and OMNIWeb NASA for providing Dst and solar data.

Authors' Contributions

All authors have the same contribution.

Data Availability

No data available.

Conflicts of Interest

The authors declare that there is no conflict of interest.

Ethical Considerations

The authors have diligently addressed ethical concerns, such as informed consent, plagiarism, data fabrication, misconduct, falsification, double publication, redundancy, submission, and other related matters.

Funding

This research did not receive any grant from funding agencies in the public, commercial, or nonprofit sectors.

References

[1] Hathaway, D. H. 2015, Living Reviews in Solar Physics, 12, 1.

[2] Garg, S., Omkar, P. T., & Saket, K., 2025, Indian Journal of Pure & Applied Physics, 63, 11.

[3] Ahmed, O., Badruddin, B., & Moncef D., 2024, Advances in Space Research, 73, 9.

[4] Watari, S., 2024, Earth, Planets and Space, 76, 137.

[5] Burton, Rande, K., McPherron, R. L., & Russell, C. T. 1975, J. Geophysical Research 80, 4204–4214.

[6] Akasofu, S. I., 1983, Space Sci. Rev., 34, 2.

[7] Joselyn, J. A., & McIntosh, P. S. 1981, J. Geophys. Res., 86, A6.

[8] Gonzalez, W. D., Joselyn, J. A., Kamide, Y., Kroehl, H. W., Rostoker, G., & et al. 1994, J. Geophys. Res. Space Phys., 99, A4.

[9] Taran, S., & et al. 2023, Advances in Space Research, 71, 12.

[10] Taran, S., Safari, H., & Daei, F., 2019, ApJ, 882, 2.

[11] Lin, J. W., 2021, European Journal of Environment and Earth Sciences, 2, 1.

[12] Abe, O. E., et al. 2023, Advances in Space Research 71, 2240.

[13] Dungey, J. W., 1961, Phys. Rev. Lett., 6, 2.

[14] Rathore, B. S., Gupta, D. C., & Kaushik, S. C., 2015, Research in Astronomy and Astrophysics, 15, 1.

[15] Wing, S., Johnson, J. R., Jen, J., Meng, C. I., Sibeck, D. G., & et al. 2005, J. Geophys. Res. Space Phys., 110, A4.

[16] Wintoft, P., Wik, M., Matzka, J., & Shprits, Y., 2017, J. Space Weather Space Clim, 7, A29.

[17] Zhelavskaya, I. S., Vasile, R., Shprits, Y. Y., Stolle, C., & Matzka, J., 2019, Space Weather, 17, 10.

[18] O'Brien, T. P. & McPherron, R. L., 2000, J. Atmospheric and Solar-Terrestrial Physics, 62.

[19] Wei, H. L., Zhu, D. Q., Billings, S. A., Balikhin, M. A., 2007, J. Atmospheric and Solar-Terrestrial Physics, Advances in Space Research, 40,12.

[20] Lazzús, J., Vega, P., Rojas, P., & Salfate, I., 2017, Space Weather, 15, 8.